



# OPEN Electrostatics-based quantum gate optimization with born scattering

Kumar Gautam<sup>1</sup> & Chang Wook Ahn<sup>2,3</sup>✉

In this paper, we propose employing electron scattering to realize unitary quantum gates that are controlled by three qubits. Using Feynman's rules, we find an expression for the transition amplitude for scattering from an external electromagnetic source. In this context, the scattering amplitude is modeled as a unitary gate whose state can be regulated. The optimal value of the vector potential needed to implement the gate is obtained by minimizing the difference between the designed gate and the target gate, with the total energy consumed as a constraint. The design algorithm is obtained by discretizing the resulting integral equations into vector equations. This design algorithm can be applied in various fields such as quantum computing, communication, and sensing. It offers a promising approach for developing efficient and accurate gates for quantum information processing. Furthermore, this approach can also be extended to design gates for multi-qubit systems, which are essential for large-scale quantum computing. The use of this algorithm can significantly contribute to the development of practical quantum technologies.

**Keywords** Quantum Gate Design, Quantum Electrodynamics, Electron Scattering, Dyson Series, Lagrange's multiplier method

In 1982, theoretical physicist Richard Feynman was the first person to talk about the idea of quantum computing<sup>1</sup>. Significant progress has been made over the past 40 years in the areas of quantum information, quantum computation, and quantum simulation, but the field as a whole has taken on new characteristics in recent years. Recent experiments have shown that scaling up the number of qubits to the dozens can lead to quantum advantage or hegemony<sup>2-4</sup>. This is close enough to most classical computers to simulate quantum bits. There is still a lot of room for improvement in the fidelity of quantum logic gates and the threshold value of quantum computing for fault tolerance, but each experimental platform is getting closer to the thousands of quantum bits needed for practical quantum computing. When considering the potential of a physical system for implementing quantum computing, it is essential to keep in mind the five requirements summarized by DiVincenzo<sup>5</sup>. DiVincenzo established criteria that must be met by any practical method of quantum computation or communication. The requirement for universal quantum gates is brought up as one of the most crucial factors. Quantum gates are the most basic building block of quantum algorithms because they are unitary operators for the evolution of quantum states in the context of the Hilbert space. Any kind of quantum computation would be impossible without universal quantum gates. DiVincenzo's criteria are now standard for determining whether or not a quantum computer is even possible. As one of DiVincenzo's five requirements for a physical system to be a viable platform for quantum computing, the availability of universal quantum gates is essential. Researchers all over the world have adopted these criteria as a standard by which to measure progress toward the goal of creating a workable quantum computer<sup>6-8</sup>.

The ability to scale up to a larger number of qubits is crucial. Many experts believe that quantum computing and quantum information will soon become the most rapidly developing areas of modern science. Research into quantum computing is ongoing, with new discoveries being made on a regular basis, such as a new kind of qubit that could increase the threshold value for fault tolerance. Practical quantum computing is a potential outcome of current technological developments<sup>9-11</sup>. For this reason, it is essential that the system be flexible enough to incorporate new findings and discoveries in the field. Since there is hope for widespread implementation of quantum computing, it is crucial that scientists and engineers keep exploring the limits of this promising new field. The efficient simulation of physical systems and the development of efficient algorithms for computational problems are two areas where quantum computing shows great promise. These computers use the quantum

<sup>1</sup>Quantum Computing Lab, Quantum Research And Centre of Excellence, New Delhi, India. <sup>2</sup>MEMI lab, AI Graduate School, Gwangju Institute of Science and Technology, Gwangju, South Korea. <sup>3</sup>GIST Institute for Artificial Intelligence (GIAI), Gwangju, South Korea. ✉email: cwan@gist.ac.kr

mechanical explanation of the universe as their foundation. The factoring problem can be solved exponentially faster using quantum mechanics, and the searching problem can be solved quadratically faster using quantum mechanics. Further, a powerful quantum algorithm for resolving linear systems of equations has been created. The study of quantum information processing has expanded as a result of these computational benefits. Quantum computers have the potential to revolutionize fields such as cryptography, drug discovery, and machine learning. However, building a reliable and scalable quantum computer remains a significant challenge in the field of quantum information processing<sup>12–16</sup>.

In quantum computing, the “qubit” is the basic building block because it defines quantum superpositions and corresponds to a quantum system with two basis states. An universal transformation is one that can be used on any other transformation in the same domain. Only unitary quantum gates are necessary to maintain the inner product between quantum states and the normalization condition of a quantum state. Another physical requirement for quantum state transformations imposed by quantum mechanics is that the evolution from the initial state to the final state must be reversible. Applications such as factorization and database searching could theoretically benefit from quantum computing’s exponential speedups over classical computing. However, challenges such as the unstable nature of quantum states and the intricacy of scaling up quantum systems make it difficult to fully realize this potential. Despite these difficulties, quantum hardware and software development has made significant strides in recent years. New algorithms and error correction techniques are being developed to lessen the impact of noise and decoherence in quantum computers with dozens of qubits. Future progress in the field may significantly alter established industries like cryptography, materials science, and pharmaceutical research<sup>16</sup>.

Unitary gates are reversible because a unitary  $U$  can be reversed by applying  $U^\dagger$ , because  $U^\dagger U = \mathbb{1}$ , that is, the identity. Various physical implementations of quantum gates have been demonstrated, based on ion traps, superconducting qubits, and nuclear magnetic resonance. However, the physical implementation of large-scale quantum computers still remains a challenge. An important categorization of quantum gates is in the form of separable and nonseparable quantum gates. Nonseparable quantum gates can not be decomposed into tensor products of gates acting on individual qubits. They include gates like CNOT, and the introduce quantum correlations between the qubits. This has important applications in the preparation of entangled states, and in quantum algorithms like phase estimation. Real quantum gates are not ideal, as they introduce errors and noise. Measures like gate fidelity and signal-to-noise ratio are used to quantify the departure of a realized gate from ideal operation. This is important from design point of view, as the amount of error introduced by a gate which can be tolerated forms a design parameter<sup>17–20</sup>.

In this paper, we use quantum electrodynamics, the quantum field theory of electron-photon interactions, to build a quantum gate. The electron is assumed to be scattered from a random potential, and the potential is obtained by minimizing the error energy between the realized gate and a given (target) unitary gate. The minimization will fail if the energy level is too high. The resulting equations are then solved using discretization and transformation to matrix equations. One such technique has been used. The design of a three-qubit controlled quantum gate that operates via electron scattering from an external electromagnetic potential is the work’s original contribution. These additional forces illuminate the nature of pair production and lambda shift. Due to the high number of degrees of freedom provided by quantum fields, they can be used to implement gates of any size. Furthermore, the optimization process determines the best external potential that can be used to compute actual physical electric and magnetic fields, bringing the realized gate as close to the target gate as possible. Because it enables the creation of larger and more complex quantum gates, this innovation has the potential to significantly improve quantum computing. Furthermore, the optimization process used in this design is applicable to other quantum gate designs, making it a significant contribution to the field of quantum computing<sup>21</sup>.

This paper contributes by investigating algorithms for resolving routing problems on quantum computers with constrained qubits using the Born approximation of scattering theory. The Born approximation is used in scattering theory, particularly quantum mechanics, to treat the incident field as the driving field rather than the total field at each point in the scattered field. In his honor, the Born approximation was named after Max Born. The perturbation method is used to consider extended body scattering. This perturbation technique stimulates the quantum system under investigation, resulting in a state transition. The significance of perturbing a quantum system with an unperturbed Hamiltonian using a weak potential stems from the ability to generate a one-dimensional Lie group of the unitary gates. As a result, the primary benefit of perturbation theory is that it enables us to increase the size of the unitary group for the gate realization of a quantum physical system from 1 to  $N$ , where  $N$  is an infinite number<sup>22</sup>. As a result, the combinatorial method can be used to convert the non-relativistic time-sliced Feynman path integral into perturbation expansions. In the current treatment, combinatorial analysis is used to generate perturbation expansions that result in path solutions for a wide range of novel settings, but there is still no practical way to derive the path integral of such space-time propagators. It allows us to assess the accuracy of numerical evaluations of path integrals that assume finite  $N$  in particular by carefully determining the impact of a finite  $N$  on a perturbation expansion of the scattering theory in the first Born approximation. Furthermore, perturbation theory is widely used in quantum field theory to calculate the interaction between particles and fields, which is critical for understanding elementary particle behavior. It’s also important in condensed matter physics, allowing us to study the behavior of many-body systems by treating their interactions as small perturbations on an idealized non-interacting system<sup>23–26</sup>.

A significant part of the complex problem is the undiscovered nature of the path optimization. Technology advancement is the key to solving this problem, and it requires careful decision making to do so. The route optimization problem can be solved with a variety of algorithms, such as deterministic, heuristic, and metaheuristic approaches. There are a few simple path problems that can be solved by each technique, but they each have their own prerequisites and limitations<sup>27</sup>.

The remainder of the paper is organized as follows: in section 2, we develop the necessary background of quantum electrodynamics, including the Dirac equation, scattering matrix, and Dyson series expansion. In section 3, we formulate the proposed model of the quantum gate, and write its transition probability amplitude using Feynman rules. In section 4, we derive the expression for total energy consumed, which is to be constrained. In section 5, we minimize the gate error energy to obtain the optimum value of vector potential, and in section 6, the design algorithm is developed via discretization. Section 7 and 8 contains the conclusion with future discussion.

## Background of quantum electrodynamics

Classical field theory interprets fields as a continuum of simple harmonic oscillators. In quantum field theory, the harmonic oscillators must be considered to be quantized in the sense that the excitation energy levels (or equivalently, frequencies) are quantized and successive energy levels differ by an energy of 1 quantum. Relativistic quantum mechanics requires a field theory viewpoint, in order to explain multiparticle states, particle-antiparticle pairs etc. A classical field can be quantized by promoting the fields and their conjugate momentum densities to operators, and imposing appropriate commutation relations. This procedure is called canonical quantization.

The real valued Klein Gordon field describes the theory of spin-0 particles, or Bosons. It has the Lagrangian density:

$$\mathcal{L} = \frac{1}{2} (\partial_\mu \phi)^2 - \frac{1}{2} m^2 \phi^2, \quad (1)$$

where  $m$  is the mass of the associated quantum. The Euler-Lagrange equation for the field gives the Klein-Gordon equation:

$$(\partial^\mu \partial_\mu + m^2) \phi = 0 \quad (2)$$

where  $\partial^\mu \partial_\mu = \frac{\partial^2}{\partial t^2} - \nabla^2$ . The canonical momentum density conjugate to  $\phi(x)$  is  $\pi(x) = \dot{\phi}(x)$ , and the Hamiltonian density is  $\mathcal{H} = \frac{1}{2} \pi^2 + \frac{1}{2} (\nabla \phi)^2 + \frac{1}{2} m^2 \phi^2$ .

In order to make Schrödinger's equation compatible with the theory of special relativity, Dirac derived an equation in which both space and time derivatives are of first order. This equation describes fermions (spin- $\frac{1}{2}$  particles) and their antiparticles, and is called the Dirac equation. The Dirac equation for a particle in an external electromagnetic field  $A_\mu(x)$  is:

$$i \gamma^\mu \partial_\mu \psi - m \psi = e \gamma^\mu A_\mu(x), \quad (3)$$

where  $\psi$  represents the state of the quantum field,  $m$  is the particle's mass and  $e$  is its charge, and  $\gamma^\mu$  represent the 4 Dirac matrices. These are  $4 \times 4$  matrices which obey the anticommutation relations

$$\{\gamma^\alpha, \gamma^\beta\} = \gamma^\alpha \gamma^\beta + \gamma^\beta \gamma^\alpha = 2 \eta^{\alpha\beta}, \quad (4)$$

where  $\eta^{\alpha\beta}$  is the Minkowski metric. In Dirac representation, they are taken as the block matrices:

$$\gamma^0 = \begin{pmatrix} \mathbb{1}_2 & \mathbb{O}_2 \\ \mathbb{O}_2 & -\mathbb{1}_2 \end{pmatrix}, \quad \gamma^j = \begin{pmatrix} \mathbb{O}_2 & \sigma^j \\ -\sigma^j & \mathbb{O}_2 \end{pmatrix}, \quad (5)$$

where  $\mathbb{1}_2$  and  $\mathbb{O}_2$  represent the  $2 \times 2$  identity matrix and matrix of zeros, respectively, and  $\sigma^j$  are the Pauli matrices for  $j = 1, 2, 3$ . They obey  $(\gamma^0)^\dagger = \gamma^0$ ,  $(\gamma^j)^\dagger = -\gamma^j$ ,  $(\gamma^0)^2 = \mathbb{1}_4$ ,  $(\gamma^j)^2 = -\mathbb{1}_4$ , for  $j = 1, 2, 3$ . Also, for a 4-vector  $c_\mu$ , Feynman's slash notation is defined as:

$$\not{c} = \gamma^\mu c_\mu. \quad (6)$$

The solutions of Dirac equation 3 for particles as well as antiparticles are 4-component objects called spinors. These solutions (in momentum space) are of the form:

$$\psi(p) = \begin{pmatrix} u^1(p) \\ u^2(p) \\ v^1(p) \\ v^2(p) \end{pmatrix} = \begin{pmatrix} u(p) \\ v(p) \end{pmatrix}, \quad (7)$$

where  $u(p)$  and  $v(p)$  represent 2-dimensional spinors. For particles at rest, the solution is of the form:

$$\psi_p(p) = \sqrt{m} \begin{pmatrix} \xi \\ \xi \end{pmatrix}, \quad (8)$$

where  $\xi$  represents the initial spin state, and for a spin up particle, it can be taken as:

$$\xi = \begin{pmatrix} 1 \\ 0 \end{pmatrix}. \quad (9)$$

For antiparticles at rest,

$$\psi_a(p) = \sqrt{m} \begin{pmatrix} \zeta \\ -\zeta \end{pmatrix}, \quad (10)$$

where  $\zeta$  for a spin up antiparticle is taken as:

$$\zeta = \begin{pmatrix} 0 \\ 1 \end{pmatrix}. \quad (11)$$

The solutions for particles and antiparticles of 4-momentum  $p^\mu$  are:

$$\psi_p(p) = \begin{pmatrix} \sqrt{p_\mu \sigma^\mu \xi} \\ \sqrt{p_\mu \bar{\sigma}^\mu \xi} \end{pmatrix}, \quad \psi_a(p) = \begin{pmatrix} \sqrt{p_\mu \sigma^\mu \zeta} \\ -\sqrt{p_\mu \bar{\sigma}^\mu \zeta} \end{pmatrix}, \quad (12)$$

respectively, where  $\sigma^\mu = (\mathbb{1}_2, \sigma_x, \sigma_y, \sigma_z)$  and  $\bar{\sigma}^\mu = (\mathbb{1}_2, -\sigma_x, -\sigma_y, -\sigma_z)$ .

Quantum electrodynamics (QED) is the quantum field theory of electron-photon interactions. The Lagrangian density for QED is:

$$\mathcal{L}_{qed} = \mathcal{L}_{dirac} + \mathcal{L}_{em} + \mathcal{L}_I, \quad (13)$$

where the Dirac (spinor) field Lagrangian density is:

$$\mathcal{L}_{dirac} = \bar{\psi} \not{\partial} \psi - \bar{\psi} m \psi. \quad (14)$$

The Lagrangian density of electromagnetism, or Maxwell Lagrangian, is:

$$\mathcal{L}_{em} = -\frac{1}{4} F_{\mu\nu} F^{\mu\nu}, \quad (15)$$

where the antisymmetric tensor  $F^{\mu\nu}$  is given by:

$$F^{\mu\nu} = \partial^\mu A^\nu - \partial^\nu A^\mu, \quad (16)$$

and the interaction term is

$$\mathcal{L}_I = -e \bar{\psi} \gamma^\mu \psi A_\mu. \quad (17)$$

Due to the interaction term, the theory is not solvable in closed form. The coupling constant for QED, which is the electronic charge  $e$ , is much smaller than one. Thus, higher order terms, which arises from higher order of interaction gives a progressively small contribution. Therefore, first order perturbation theory gives a highly precise description of QED. The probability amplitudes of interaction processes are given by the scattering matrix elements<sup>28-30</sup>.

Scattering theory involves free particle states coming in at  $t = -\infty$ , undergoing interaction and going out as different free particle states at  $t = \infty$ . Such a process must conserve the 4-momentum. Consider an initial state  $|\psi_i(t_1)\rangle$  which evolves according to a unitary transformation  $\hat{U}(t_2, t_1)$ . The amplitude to evolve to the final state  $|\psi_f(t_2)\rangle$  is given by  $\langle \psi_f(t_2) | \hat{U}(t_2, t_1) | \psi_i(t_1) \rangle$ . The scattering matrix element is given by:

$$S_{fi} = \lim_{\substack{t_1 \rightarrow -\infty \\ t_2 \rightarrow \infty}} \langle \psi_f(t_2) | \hat{U}(t_2, t_1) | \psi_i(t_1) \rangle \quad (18)$$

This scattering matrix element is proportional to the transition probability amplitude between the initial and final states.

Scattering phenomena can be studied in the interaction picture of quantum mechanics. In this, the Hamiltonian is written as a sum of two terms: the free Hamiltonian  $\hat{H}_0$  and a time-dependent interaction component  $\hat{H}_I$ . The states in interaction picture evolve as:

$$i \frac{\partial}{\partial t} |\psi_I(t)\rangle = \hat{H}_I |\psi_I(t)\rangle \quad (19)$$

i.e., according to the interaction Hamiltonian. On the other hand, an operator  $\hat{O}_I$  evolves according to the free Hamiltonian:

$$\frac{\partial}{\partial t} \hat{O}_I = [\hat{H}_0, \hat{O}_I] \quad (20)$$

In this picture, the unitary evolution operator for time evolution of interaction picture states obeys:

$$i \frac{\partial}{\partial t} \hat{U}_I(t, t_0) = \hat{H}_I(t) \hat{U}_I(t, t_0), \quad \hat{U}_I(t_0, t_0) = \mathbb{1}, \quad (21)$$

where

$$\hat{H}_I(t) = e^{i\hat{H}_0(t-t_0)} \hat{H}_I(t_0) e^{-i\hat{H}_0(t-t_0)} \quad (22)$$

The solution to this equation is the Dyson series:

$$\hat{U}_I(t, t_0) = \mathbb{1} + \sum_{n=1}^{\infty} \frac{(-i)^n}{n!} \int_{t_0}^t dt_n dt_{n-1} \cdots dt_1 \mathbf{T} [\hat{H}_I(t_n) \hat{H}_I(t_{n-1}) \cdots \hat{H}_I(t_1)] \quad (23)$$

where  $\mathbf{T}[\cdot]$  represents time ordering. Compactly, the Dyson series can be written as:

$$\hat{U}_I(t, t_0) = \mathbf{T} \left[ e^{-i \int_{t_0}^t d\tau \hat{H}_I(\tau)} \right]. \quad (24)$$

From this expression for the unitary evolution, the scattering matrix is derived as:

$$\hat{S} = \hat{U}_I(t \rightarrow \infty, t_0 \rightarrow -\infty) = \mathbf{T} \left[ e^{-i \int_{-\infty}^{\infty} d^4 y \hat{H}_I(y)} \right], \quad (25)$$

A large-size quantum unitary gate, such as the quantum Fourier transform gate, can be designed using methods that involve perturbing the field's Hamiltonian density with quantum field theoretic potentials and then matching the unitary dynamics of this evolution with a specific unitary gate. It has also been brought up that the Born-Feynman approach can be used to design large-scale unitary quantum gates. This is accomplished by recording the scattering matrix for two-electron scattering, with an external field of control included. By modifying the external control field, we are able to align this scattering matrix with a desired matrix, and the electron and photon propagators are utilized in the evaluation of this diagram. The Feynman diagrams for each type of scattering process can be assessed using the Dyson series terms for the evolution operator<sup>32</sup>. The S-matrix for a specific interaction will be provided in terms of the control parameters in each Feynman diagram. Subsequently, we can select these parameters to ensure that the computed S-matrix is as close as possible to a prescribed S-matrix in relation to an appropriately selected norm on the space of matrices. The scattering matrix is denoted as the unitary evolution operator for a time-dependent Hamiltonian over the time interval  $(-\infty, \infty)$  in Eq. 25.

The unitary evolution operator is the solution to Schrodinger's equation and is represented as the time-ordered version of the exponential of the Hamiltonian over the entire time interval. Once we adopt the interaction picture of Dirac, the Dyson series is the result. In this model, observables change based on the unperturbed time-independent Hamiltonian, which is the total Hamiltonian for fields that don't interact with each other. On the other hand, states change based on the time-dependent interaction Hamiltonian, which is the change that happens when the unperturbed Hamiltonian's value is rotated over time. It is possible to express the scattering matrix  $\hat{S}$  as a Dyson series expansion in terms of the time-dependent interaction Hamiltonian  $H(t)$ . The Dyson series should be truncated at some order  $n$  to approximate  $\hat{S}$  as a unitary operator  $U(t)$  that operates in finite time. The expression  $U(t)$  should be derived explicitly in terms of  $H(t)$  integrated over a finite interaction time  $t$ . Present the argument that higher-order terms in the Dyson series will be insignificant for sufficiently short " $t$ ", thereby justifying the truncation of the series. Give an estimate of the maximum amount of time, denoted by  $t$ , beyond which the approximation becomes breaks down. To demonstrate that  $U(t)$  is a valid approximation, it is necessary to demonstrate that it reduces to the true S in the limit  $t \rightarrow \infty$ .

That is,

$$\hat{S} = \mathbf{T} \left[ \mathbb{1} - i \int d^4 y \hat{H}_I(y) + \frac{(-i)^2}{2} \int d^4 y_1 d^4 y_2 \hat{H}_I(y_1) \hat{H}_I(y_2) + \cdots \right], \quad (26)$$

where  $\hat{H}_I(y)$  represents the interaction Hamiltonian density at spacetime point  $y$ . A Feynman diagram can be viewed as a space-time diagram representing an interaction process. The series in Eq.26 is a perturbative expansion for the scattering matrix, where each term can be interpreted as a Feynman diagram, by virtue of Wick's theorem. This theorem states that the vacuum expectation value of the Time ordered product of field operators is equal to the sum of vacuum expectation of their normally ordered versions and all possible contractions. These contraction terms of a given order can be identified with various interaction diagrams, and their transition amplitudes can be written with the help of Feynman rules.

### Formulation of the proposed unitary gate

Writing the transition amplitude for the proposed gate requires the following definitions. The Dirac adjoint of a spinor field  $\psi$ , denoted as  $\bar{\psi}$ , is defined as  $\bar{\psi} = \psi^\dagger \gamma^0$ , where  $\psi^\dagger$  is the transpose conjugate. This is defined in this manner because  $\bar{\psi}\psi$  is Lorentz invariant, whereas the quantity  $\psi^\dagger\psi$  is not. Similarly, the Dirac adjoint of a  $4 \times 4$  matrix is defined as  $\bar{M} = \gamma^0 M^\dagger \gamma^0$ . Also,  $\bar{M} = M$  and  $\bar{\gamma}^\mu = \gamma^\mu$ .

The Feynman rules to write down transition amplitudes for quantum electrodynamics (in momentum space) are as follows: an incoming fermion of 4-momentum  $p$  and helicity  $\sigma$  contributes to a term  $u(p, \sigma)$ , which is its state in spinor representation. The same is true for an outgoing antifermion. An incoming antifermion (shown with an arrow with reversed direction) contributes  $\bar{u}(p, \sigma)$ , as also an outgoing fermion. External photons lead to polarization terms of the form  $\epsilon_\mu(k)$ . According to Feynman, interaction with a photon coming from a source of 4-potential  $A_\mu(x)$  requires a term  $(-ie\gamma^\mu) a_\mu(k)$ , where  $a_\mu(k)$  is the Fourier transform of 4-potential:

$$A_\mu(x) = \int a_\mu(k) e^{-ik \cdot x} d^4k. \tag{27}$$

This follows from the solution of the inhomogeneous Dirac equation, containing the external electromagnetic potential. Vertices are points of interaction in spacetime, and contribute

$$-ie\gamma^\mu \times \delta^{(4)} \left( \sum_{in} (p) - \sum_{out} (p) \right). \tag{28}$$

The 4-dimensional delta function enforces conservation of 4-momentum. The transition of a particle from one point to another leads to the inclusion of a propagator, or the two-point correlation function. Here, the electron propagator for momentum  $p$  is denoted by  $S(p)$ . The momentum of such an internal particle is undetermined, so the amplitude has to be integrated over this momentum.

The proposed gate is designed as follows: The state of qubits is assumed to be encoded in the momentum and helicity of incoming and outgoing electrons, and the unitary gate is required to perform the necessary transition between these states. An incoming electron of state  $u_{in}(p, \sigma)$  interacts with an external photon coming from the potential  $A_\mu(x)$  (or  $a_\mu(k)$ ). The electron is scattered and now has momentum  $p + k$ , and after propagation, loses a photon of momentum  $k' = p + k - p'$  and polarization  $s'$ . The outgoing electron has the state  $\bar{u}_{out}(p', \sigma')$ . The complementary process in which the electron loses a photon before getting scattered is indistinguishable from the scattering process just described, and contributes to the probability amplitude as well. The Feynman diagram for both the processes is illustrated in Fig. 1 respectively, with time progressing vertically upwards. Here, we have considered only the lowest order process; contributions from self loop terms and vacuum polarization effects induced by external electromagnetic fields can also be included<sup>18–34</sup>.

Following the rules given by Feynman, the transition amplitude for the first diagram in Fig.1 can be written as:

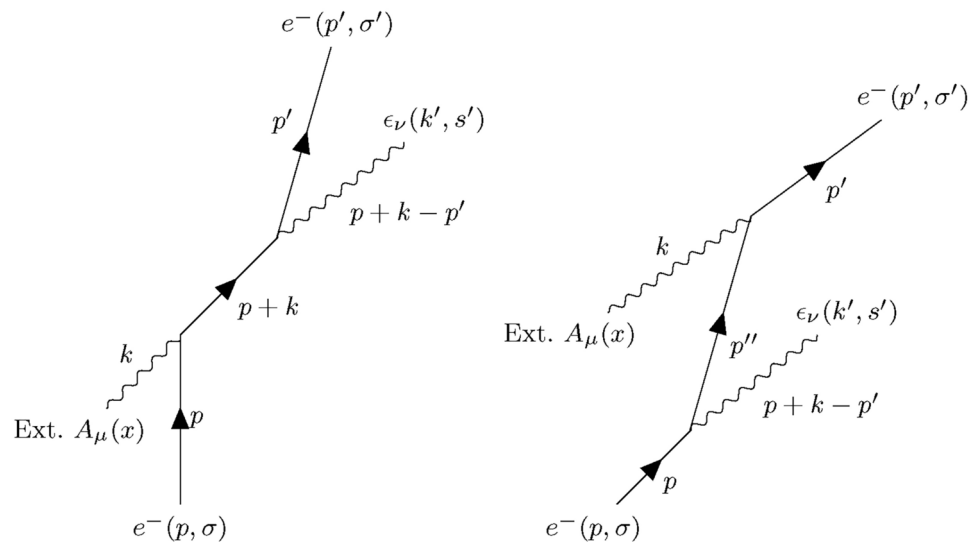


**Figure 1.** Feynman diagrams for the scattering of an electron from an external potential, used to realize the unitary quantum gate. Both processes are indistinguishable. In the second diagram, Here,  $p'' = p - k$ .

$$X_{(1)}(p', \sigma' | p, \sigma) = \int_{\Omega_{\min} \leq |k| \leq \Omega_{\max}} \frac{(2\pi)^4}{\iota} \frac{1}{2} \sum_{s'} \bar{u}_{\text{out}}(p', \sigma') \epsilon_\nu(p+k-p', s') (-\iota e \gamma^\nu) \cdots \cdots S(p+k) (-\iota e \gamma^\mu) a_\mu(k) u_{\text{in}}(p, \sigma) d^3 k. \tag{29}$$

The complex conjugate of this amplitude, denoted by  $X_{(1)}^*$ , is formed by the following consideration: if  $a, b$  represent spinors and  $M_1, \dots, M_n$  represent  $4 \times 4$  matrices, then the complex conjugate of the scalar  $(\bar{b} M_1, \dots, M_n a)$  is given by:

$$(\bar{b} M_1, \dots, M_n a)^* = \bar{a} \bar{M}_n \cdots \bar{M}_1 b = \bar{a} \gamma^0 M_n^\dagger \cdots M_1^\dagger \gamma^0 b. \tag{30}$$

Thus,

$$X_{(1)}^*(p', \sigma' | p, \sigma) = \int_{\Omega_{\min} \leq |\mathcal{K}| \leq \Omega_{\max}} \frac{(2\pi)^4}{-\iota} \frac{1}{2} \sum_{s''} \bar{u}_{\text{in}}(p, \sigma) \gamma^0 a_\beta^*(\mathcal{K}) (\iota e (\gamma^\beta)^\dagger) S^\dagger(p+\mathcal{K}) \cdots \cdots (\iota e (\gamma^\alpha)^\dagger) \epsilon_\alpha^*(p+\mathcal{K}-p', s'') \gamma^0 u_{\text{out}}(p', \sigma') d^3 \mathcal{K}. \tag{31}$$

Similarly, the amplitude and its complex conjugate for the second diagram in Fig.1 are given by:

$$X_{(2)}(p', \sigma' | p, \sigma) = \int_{\Omega_{\min} \leq |k| \leq \Omega_{\max}} \frac{(2\pi)^4}{\iota} \frac{1}{2} \sum_{s'} \bar{u}_{\text{out}}(p', \sigma') (-\iota e \gamma^\mu) a_\mu(k) S(p'-k) \cdots \cdots (-\iota e \gamma^\nu) \epsilon_\nu(p+k-p', s') u_{\text{in}}(p, \sigma) d^3 k, \tag{32}$$

and

$$X_{(2)}^*(p', \sigma' | p, \sigma) = \int_{\Omega_{\min} \leq |\mathcal{K}| \leq \Omega_{\max}} \frac{(2\pi)^4}{-\iota} \frac{1}{2} \sum_{s''} \bar{u}_{\text{in}}(p, \sigma) \gamma^0 \epsilon_\alpha^*(p+k-p', s'') (\iota e (\gamma^\alpha)^\dagger) \cdots \cdots S^\dagger(p'-\mathcal{K}) (\iota e (\gamma^\beta)^\dagger) a_\beta^*(\mathcal{K}) \gamma^0 u_{\text{out}}(p', \sigma') d^3 \mathcal{K}, \tag{33}$$

respectively.

For simplification, the amplitudes in Eq.29 and Eq.30 may be expressed as:

$$X_{(1)}(p', \sigma' | p, \sigma) = \int_{\Omega_{\min} \leq |k| \leq \Omega_{\max}} \Gamma_{(1)}^\mu(p', \sigma' | p, \sigma; k) a_\mu(k) d^3 k, \tag{34}$$

and

$$X_{(1)}^*(p', \sigma' | p, \sigma) = \int_{\Omega_{\min} \leq |k| \leq \Omega_{\max}} \left( \Gamma_{(1)}^\beta(p', \sigma' | p, \sigma; \mathcal{K}) \right)^* a_\beta^*(\mathcal{K}) d^3 \mathcal{K}, \tag{35}$$

where

$$\Gamma_{(1)}^\mu(p', \sigma' | p, \sigma; k) = \frac{(2\pi)^4}{\iota} \frac{1}{2} \sum_{s'} \bar{u}_{\text{out}}(p', \sigma') \epsilon_\nu(p+k-p', s') (-\iota e \gamma^\nu) S(p+k) (-\iota e \gamma^\mu) u_{\text{in}}(p, \sigma). \tag{36}$$

Similarly,

$$X_{(2)}(p', \sigma' | p, \sigma) = \int_{\Omega_{\min} \leq |k| \leq \Omega_{\max}} \Gamma_{(2)}^\mu(p', \sigma' | p, \sigma; k) a_\mu(k) d^3 k, \tag{37}$$

and

$$X_{(2)}^*(p', \sigma' | p, \sigma) = \int_{\Omega_{\min} \leq |k| \leq \Omega_{\max}} \left( \Gamma_{(2)}^\beta(p', \sigma' | p, \sigma; \mathcal{K}) \right)^* a_\beta^*(\mathcal{K}) d^3 \mathcal{K}, \tag{38}$$

with

$$\Gamma_{(2)}^\mu(p', \sigma'|p, \sigma; k) = \frac{(2\pi)^4}{\iota} \frac{1}{2} \sum_{s'} \bar{u}_{\text{out}}(p', \sigma') (-\iota e \gamma^\mu) S(p' - k) (-\iota e \gamma^\nu) \epsilon_\nu(p + k - p', s') u_{\text{in}}(p, \sigma). \tag{39}$$

The total probability amplitude,  $X$ , for the process would be

$$X(p', \sigma'|p, \sigma) = X_{(1)}(p', \sigma'|p, \sigma) + X_{(2)}(p', \sigma'|p, \sigma). \tag{40}$$

### Energy considerations

Here we derive the expression for total energy of the external source, under whose influence the electron is undergoing scattering. Consider the 4-potential  $A_\mu(x) = (0, \vec{A}(x))$ , and its Fourier transform as  $a_\mu(k) = (0, \vec{a}(k))$ . The arrow over the symbol denotes a vector in 3 dimensions. We will impose the radiation gauge conditions, i.e.  $\nabla^\mu A_\mu(x) = 0$ , which, in frequency domain, is:

$$\vec{k} \cdot \vec{a}(k) = 0. \tag{41}$$

Also, for the photons mediating the interaction of electrons with the potential, the 4-momentum can be taken to be  $(k^0, \vec{k})$ , where  $k^0 = |\vec{k}|$ . We will also assume that the source can only emit photons whose momenta are bounded by  $\Omega_{\text{min}}$  and  $\Omega_{\text{max}}$ , i.e.,  $\Omega_{\text{min}} \leq |\vec{k}| \leq \Omega_{\text{max}}$ .

The electric field (in time domain) is given by:

$$\vec{E} = -\frac{\partial \vec{A}}{\partial t} - \nabla A^0, \tag{42}$$

which, in frequency domain, becomes

$$\vec{E}(k) = -\iota k^0 \vec{a}(k). \tag{43}$$

The energy stored in the electric field can be calculated as:

$$\epsilon_{\text{elec}} = \frac{1}{2} \epsilon_0 \int |\vec{E}|^2 d^3x = \frac{1}{2} \frac{1}{(2\pi)^3} \epsilon_0 \int |\vec{E}(\vec{k})|^2 d^3k, \tag{44}$$

where the second equality follows from Parseval's theorem. Substituting from Eq.43,

$$\epsilon_{\text{elec}} = \frac{1}{2} \frac{1}{(2\pi)^3} \epsilon_0 \int (k^0)^2 |-\iota \vec{a}(k)|^2 d^3k = \frac{1}{2} \frac{1}{(2\pi)^3} \epsilon_0 \int |\vec{k}|^2 |\vec{a}(k)|^2 d^3k. \tag{45}$$

Also, in time domain, the magnetic field,  $\vec{B}$ , is given by:

$$\vec{B} = \nabla \times \vec{A}(t), \tag{46}$$

which, in frequency domain, is:

$$\vec{B} = \iota \vec{k} \times \vec{a}(k). \tag{47}$$

Using the vector identity

$$|\vec{k} \times \vec{a}(k)|^2 = |\vec{k}|^2 |\vec{a}(k)|^2 - |\vec{k} \cdot \vec{a}(k)|^2 = |\vec{k}|^2 |\vec{a}(k)|^2, \tag{48}$$

where the second equality follows from Eq.41. Thus, the energy in the magnetic field is:

$$\epsilon_{\text{mag}} = \frac{1}{2\mu_0} \int |\vec{B}|^2 d^3x = \frac{1}{2\mu_0} \int |\vec{k} \times \vec{a}(k)|^2 d^3k = \frac{1}{2\mu_0} \frac{1}{(2\pi)^3} \int |\vec{k}|^2 |\vec{a}(k)|^2 d^3k. \tag{49}$$

We want the sum of energies stored in electric and magnetic fields to be equal to a fixed energy  $\epsilon'_{\text{max}}$ . Thus,

$$\epsilon'_{\text{max}} = \epsilon_{\text{elec}} + \epsilon_{\text{mag}} = \frac{1}{2(2\pi)^3} \left( \epsilon_0 + \frac{1}{\mu_0} \right) \int |\vec{k}|^2 |\vec{a}(k)|^2 d^3k, \tag{50}$$

and we can absorb the constants into the quantity  $\epsilon_{\text{max}}$ , and equivalently write:

$$\varepsilon_{\max} = \int |\vec{k}|^2 |\vec{a}(k)|^2 d^3k. \tag{51}$$

This is the energy constraint. These integrals will be evaluated in the interval  $\Omega_{\min} \leq |\vec{k}| \leq \Omega_{\max}$ .

### Gate error energy and optimization

The target unitary gate, i.e. the gate to be designed is assumed as  $G(p', \sigma'|p, \sigma)$ . The gate error energy is used to quantify the difference between the realized gate and the target gate, and we choose the following form:

$$\sum_{\sigma, \sigma'} \int (X - G)(X^* - G^*) d^4p d^4p' \tag{52}$$

and together with the energy constraint Eq.51, the optimization problem is cast as:

$$P : \underset{a_\mu(k)}{\text{minimize}} \sum_{\sigma, \sigma'} \int (X - G)(X^* - G^*) d^4p d^4p', \tag{53}$$

subject to  $\int |\vec{k}|^2 |\vec{a}(k)|^2 d^3k = \varepsilon_{\max}$ .

Thus, the required functional  $\mathcal{Z}$  is constructed as:

$$\mathcal{Z}(a_\mu(k), a_\beta^*(\mathcal{K}), \lambda) = \sum_{\sigma, \sigma'} \int (X - G)(X^* - G^*) d^4p d^4p' - \lambda \left( \int |\vec{k}|^2 |\vec{a}(k)|^2 d^3k - \varepsilon_{\max} \right) \tag{54}$$

Here,  $\lambda$  is the Lagrange's multiplier.

For the minimization, we re-write the energy constraint as:

$$\begin{aligned} \varepsilon_{\max} &= \int |\mathcal{K}|^2 |\vec{a}(\mathcal{K})|^2 d^3\mathcal{K} \\ &= \int |\vec{\mathcal{K}}|^2 a_\mu(\mathcal{K}) a^{*\mu}(\mathcal{K}) d^3\mathcal{K} \\ &= \int |\vec{\mathcal{K}}|^2 a_\mu(\mathcal{K}) a_\beta^*(\mathcal{K}) \eta^{\mu\beta} d^3\mathcal{K}, \end{aligned} \tag{55}$$

where  $\eta^{\mu\beta}$  is the Minkowski metric. The aim is to multiply the terms in Eq.52 to express them as quadratic, linear and constant terms in terms of 4- potential. That is, using Eq.34-38 we simplify Eq.52 to obtain  $\mathcal{Z}$  in the form:

$$\begin{aligned} \mathcal{Z} &= \int a_\mu(k) a_\beta^*(\mathcal{K}) \Psi^{\mu\beta} d^3k d^3\mathcal{K} + \int a_\mu(k) \chi^\mu d^3k + \int a_\beta^*(\mathcal{K}) (\chi^\beta)^* d^3\mathcal{K} \\ &\quad - \lambda \int |\vec{\mathcal{K}}|^2 a_\mu(\mathcal{K}) a_\beta^*(\mathcal{K}) \eta^{\mu\beta} d^3\mathcal{K} + \lambda \varepsilon_{\max} + \int G G^* d^4p d^4p' \end{aligned} \tag{56}$$

where

$$\Psi^{\mu\beta} = \int (\Gamma_{(1)}^\mu + \Gamma_{(2)}^\mu) \left( (\Gamma_{(1)}^\beta)^* + (\Gamma_{(2)}^\beta)^* \right) d^4p d^4p', \tag{57}$$

and

$$\chi^\mu = - \int G^* (\Gamma_{(1)}^\mu + \Gamma_{(2)}^\mu) d^4p d^4p'. \tag{58}$$

Now, we differentiate  $\mathcal{Z}$  by treating  $a_\mu(k)$  and  $a_\beta^*(\mathcal{K})$  as separate variables, i.e. setting

$$\frac{\partial \mathcal{Z}}{\partial a_\beta^*(\mathcal{K})} = 0 \tag{59}$$

yields

$$\int a_\mu(k) \Psi^{\mu\beta} d^3k + (\chi^\beta)^* - \lambda \int |\vec{\mathcal{K}}|^2 a_\mu(\mathcal{K}) \eta^{\mu\beta} = 0, \tag{60}$$

i.e.

$$\int \left( \Psi^{\mu\beta} - \lambda |k|^2 \delta^3(\vec{k} - \vec{K}) \eta^{\mu\beta} \right) a_\mu(k) d^3k = -(\chi^\beta)^*. \quad (61)$$

This is the result of the minimization, and the solution to these equations will give the optimal value of  $a_\mu(k)$  (and hence  $A_\mu(x)$ ) required to design the gate.

### Discretization and the design algorithm

For the discretization of photon momentum space, take

$$\vec{k} = \frac{\vec{r}}{M} \text{ and } \vec{K} = \frac{\vec{s}}{M}, \quad (62)$$

where  $M$  is a large number. The components of  $\vec{r} = (r_x, r_y, r_z)$  and  $\vec{s} = (s_x, s_y, s_z)$  are assumed to vary in integer increments, subject to  $\Omega_{\min} \leq |\vec{k}|, |\vec{K}| \leq \Omega_{\max}$ . The differential volume element  $d^3k$  is replaced by  $\frac{1}{M^3}$ .

. Then, the discretized version of Eq.61 becomes:

$$\frac{1}{M^3} \left[ \sum_{\vec{r}} \left( \Psi^{\mu\beta}(\vec{r}, \vec{s}) - \lambda \left| \frac{\vec{r}}{M} \right|^2 \delta^{(3)}(\vec{r} - \vec{s}) \eta^{\mu\beta} \right) a_\mu(\vec{r}) \right] = -(\chi^\beta)^*(\vec{s}), \quad (63)$$

where the summation is over  $\vec{r}$  such that  $\Omega_{\min} \leq \left| \frac{\vec{r}}{M} \right| \leq \Omega_{\max}$ . These are equations for all values of  $\vec{s}$  and  $\beta$ .

. To solve these, we convert them into matrix form as follows: Let  $\mathbf{S}$  be the matrix formed by  $\frac{1}{M^3} \Psi^{\mu\beta}(\vec{r}, \vec{s})$ , indexed by  $\vec{r}$  and  $\vec{s}$ . The indexing is carried out by introducing a lexicographic ordering. Similarly,  $\mathbf{D}$  is the diagonal matrix formed by the terms  $\frac{1}{M^3} \left| \frac{\vec{r}}{M} \right|^2 \delta^{(3)}(\vec{r} - \vec{s}) \eta^{\mu\beta}$ . Also, let  $\mathbf{a}$  and  $\mathbf{c}$  be vectors formed by  $a_\mu(\vec{r})$  and  $(\chi^\beta)^*(\vec{s})$ , respectively. Then the matrix-vector equation is:

$$(\mathbf{S} - \lambda \mathbf{D}) \mathbf{a} = -\mathbf{c}, \quad (64)$$

which can be solved for  $\mathbf{a}$  as:

$$\mathbf{a} = -(\mathbf{S} - \lambda \mathbf{D})^{-1} \mathbf{c}. \quad (65)$$

However, this still requires the value of  $\lambda$ . For that, use the discrete version of energy constraint, Eq.51, as:

$$\mathbf{a}^\dagger \mathbf{D} \mathbf{a} = \varepsilon_{\max}. \quad (66)$$

Substitute from 65 to get:

$$\mathbf{c}^\dagger \left( (\mathbf{S} - \lambda \mathbf{D})^{-1} \right)^\dagger \mathbf{D} (\mathbf{S} - \lambda \mathbf{D})^{-1} \mathbf{c} = \varepsilon_{\max}. \quad (67)$$

This equation is hard to solve for  $\lambda$ . So, an iterative algorithm is developed: choose a guess for  $\lambda$ , say  $\lambda^{(0)}$ , and solve iteratively as:

$$\mathbf{a}^{(n+1)} = -\left( \mathbf{S} - \lambda^{(n)} \mathbf{D} \right)^{-1} \mathbf{c} \quad (68)$$

and

$$\left( \mathbf{S} - \lambda^{(n+1)} \mathbf{D} \right) \mathbf{a}^{(n+1)} = -\mathbf{c}. \quad (69)$$

Solving this for  $\lambda^{(n+1)}$  gives

$$\lambda^{(n+1)} = \frac{\mathbf{a}^{\dagger(n+1)} (\mathbf{S} \mathbf{a}^{(n+1)} + \mathbf{c})}{\mathbf{a}^{\dagger(n+1)} \mathbf{D} \mathbf{a}^{(n+1)}}. \quad (70)$$

The aim is to solve the equations Eq.68-70 to obtain the vector potential of the scattering center, which would implement the required unitary gate as closely as possible to the target unitary gate.

### Conclusion

In this paper, an external c-number valued electromagnetic four potential is applied as input to the Compton scattering problem, and using the Feynman diagrammatic rules, we evaluate the scattering probability amplitude

of an electron which first absorbs and then re-emits a photon in the presence of the control input electromagnetic field. The total scattering probability amplitude also includes the amplitude of the process in which the incoming electron first loses a photon and then undergoes scattering by the external potential. This scattering amplitude is treated as a controlled unitary gate, whose matrix elements are indexed by row index  $(p, \sigma)$  and column index  $(p', \sigma')$ , where  $(p, \sigma)$  are the initial 4-momentum and spin of the electron, and  $(p', \sigma')$  are the final 4-momentum and spin of the electron, respectively. The controlling external electromagnetic potential  $a_\mu$  is then selected so that this controlled unitary gate is as close as possible to a given unitary gate in the Frobenius/Hilbert-Schmidt norm. The norms are evaluated in MATLAB by discretizing the momentum variables and replacing continuous momentum integrals by discrete momentum sums.

As future scope of study, this method could be applied to non-relativistic condensed matter systems described by quantum field theory, and these could be used to develop practical quantum gates. These questions will be addressed in a future work.

### Discussion of future work

Surprisingly, complex issues can be avoided through the use of scattering matrix theory. Feynman's method was effective because it predicted that the well-known divergences in a S matrix would cancel each other out. When considering the long-term future of electrodynamics, it is necessary to take into account the fact that divergences spontaneously disappear. The fact that the theory is based on an infinite interaction function within a Hamiltonian formalism, which is incompatible with the finiteness of the S matrix, further undermines its physical validity. This work makes extensive use of mathematics, with a primary focus on the outcomes that can be anticipated by strictly adhering to certain mathematical formalities. To evaluate their future significance, one must switch from mathematics to physics terminology. Assuming that the mathematical formalism has relevance to natural phenomena is the first step in reconciling the seemingly inconsistent results. Future electrodynamics must rely solely on physical constants and be free of infinite regressions. Future experiments and our growing understanding of the interconnections between electrodynamics, meson phenomena, and nuclear phenomena will help to further refine this theory. Although the statement remains false, it is no longer completely false. It is essential to develop this theory so that we can comprehend the rules of nature and the subatomic behavior of matter. More research and experimentation could result in new insights into the operation of the universe. As we discover new techniques for manipulating and utilizing subatomic particles, continued investigation of this theory could also lead to technological advancements in fields such as energy and medicine. To unlock the full potential of our understanding of the subatomic world, it is essential that we continue to invest in research and development in this area.

#### Remarks: Trace-Preserving Completely Positive (TPCP) map-based Born-Feynman path integral quantum gate design

$$\mathcal{C}(\text{CNOT}) = \begin{cases} |c\rangle \otimes |t\rangle & \text{if } |c\rangle = |0\rangle \\ |c\rangle \otimes |t \oplus 1\rangle & \text{if } |c\rangle = |1\rangle \end{cases} \quad (71)$$

$$\mathcal{A}_{\text{CNOT}} = \int \mathcal{D}[\phi_c] \mathcal{D}[\phi_t] e^{iS[\phi_c, \phi_t]} \langle \psi_f | \phi_c \otimes \phi_t | \psi_i \rangle \quad (72)$$

Our subsequent research will concentrate on the Hilbert space in which the quantum field's state undergoes unitary evolution. We study techniques for controlling this evolution and develop TPCP maps from the quantum evolution of the fields. For the fields, the Feynman path integral formula is the source of the wave functional or TPCP maps' evolution. By combining non-demolition noise measurements with quantum stochastic filtering techniques, we can approximate the fields' evolving states. We create a set of time-evolving maps using these estimations to bring the TPCP map outputs into line with the estimated evolving state. Because of this, we can model the changing state of the quantum noisy fields. It is essential to acknowledge that it is impossible to directly match the designed TPCP map to yield the exact evolving system state. This limitation is due to the fact that the evolving state can only be estimated using non-demolition measurements, and it is impossible to definitively determine the evolving state.

The following factors are assessed in the design of unitary or TPCP gates that closely approximate specific unitary or TPCP gates: The TPCP gate operates in a lower dimensional Fock space than the original unitary gate. Partial tracing over the scalar and gaugino fields is the method by which the TPCP gate is obtained, which also involves path integration. These methods can be used to identify control parameters that produce a unitary gate or TPCP gate that is as close as possible to the target gate. When designing TPCP gates, a comprehensive analysis of the most suitable truncation and approximation techniques is performed. The gate design is optimized in response to the influence of truncated fields on the gate behavior that we investigate. Estimating the changing state necessitates non-demolition measurements. We compare the estimated evolving state obtained from these measurements to the outputs of the designed TPCP gate. During this matching process, the TPCP gate's parameters are adjusted to reduce the discrepancy between the estimated state and the gate's output. The gate design and matching process can be defined as an optimization problem with the goal of reducing the distance between the desired gate and the designed gate. The objective of our methodology is to create unitary or TPCP gates that closely resemble the target gates while also considering the constraints imposed by partial tracing and estimation processes. Specific implementation details and techniques will be implemented in accordance with the specific system and problem requirements.

## Data availability statement

This published article contains all of the data generated or analyzed during this study.

Received: 27 June 2023; Accepted: 15 October 2024

Published online: 28 October 2024

## References

1. Feynman, R.P.: Simulating Physics with Computers, International Journal of Theoretical Physics, Vol.21, Nos. 6/7 (1982).
2. Deutsch, D. Quantum Theory, the Church-Turing Principle and the Universal Quantum Computer. *Proceedings of the Royal Society of London A* **400**, 97–117 (1985).
3. Shor, W. Polynomial-Time Algorithms for Prime Factorization and Discrete Logarithm on a Quantum Computer. *SIAM J. Comput.* **26**(5), 1484–1509 (1997).
4. Cleve, R., Ekert, A., Macchiavello, C. & Mosca, M. Quantum algorithms revisited. *Proc. R. Soc. Lond. A* **454**, 339 (1998).
5. DiVincenzo, D. P. Two-bit gates are universal for quantum computation. *Phys. Rev. A* **51**, 1015 (1995).
6. Cheung, D.: Using Generalized Quantum Fourier Transforms in Quantum Phase Estimation Algorithms, University of Waterloo (2003).
7. Harrow, A. W., Hassidim, A. & Lloyd, S. Quantum Algorithm for Solving Linear Systems of Equations. *Phys. Rev. Lett.* **15**(103), 150502 (2009).
8. Nielsen, M. A. & Chuang, I. L. *Quantum Computation and Quantum Information* (Cambridge Univ. Press, 2000).
9. Dirac, P.A.M.: The Principles of Quantum Mechanics, Oxford University Press, 4th edition, pp. 108–178, (1958).
10. Schiff, Leonard I.: Quantum Mechanics, McGraw-Hill, 3rd edition, pp.19–279 (1968).
11. Kato, T. *Perturbation Theory for Linear Operators* 2nd edn. (Springer-Verlag, Berlin Heidelberg New York, 1980).
12. Griffiths, D.J.: Introduction to Quantum Mechanics, Pearson Hall, 2nd edition, (2005).
13. Perelomov, A. M.: Generalized Coherent States and their Applications, Texts and Monographs in Physics. Springer-Verlag, 7–39, (1986).
14. Zhang, W., Feng, D., Gilmore, R.: Coherent States - Theory and some Applications, Rev. of Modern Physics, pp. 867–927, no. 62, (1990).
15. Ralph, T. C., Gilchrist, A., Milburn, G. J., Munro, W. J. & Glancy, S. Quantum Computation with Optical Coherent States. *Phys. Rev. Lett. A* **68**, 042319 (2003).
16. Gautam, K., Rawat, T. K., Parthasarathy, H. & Sharma, N. Realization of Commonly Used Quantum Gates Using Perturbed Harmonic Oscillator. *Quantum Information Processing* **14**(9), 3257–3277 (2015).
17. Parthasarathy, H. *Mathematical Ideas for Signal Processing Applications* (I.K. International Pub. House Pvt, Ltd, 2013).
18. Gautam, K., Chauhan, G., Rawat, T. K., Parthasarathy, H. & Sharma, N. Realization of Quantum Gates Based on Three-Dimensional Harmonic Oscillator in a Time-Varying Electromagnetic Field. *Quantum Information Processing* **14**(9), 3279–3302 (2015).
19. Sharma, N., Rawat, T. K., Parthasarathy, H. & Gautam, K. Realization of a Quantum Gate Using Gravitational Search Algorithm by Perturbing Three-Dimensional Harmonic Oscillator with an Electromagnetic Field. *Quantum Information Processing* **15**, 2275 (2016).
20. Gautam, K., Rawat, T. K., Parthasarathy, H., Sharma, N. & Upadhyaya, V. Realization of the Three-Qubit Quantum Controlled Gate Based on Matching Hermitian Generators. *Quantum Information Processing* **16**(5), 113 (2017).
21. Altafini, C., On the Generation of Sequential Unitary Gates From Continuous Time *Schrödinger* Equations Driven by External Fields, *Quantum Information Processing*, pp.207–224, 1(2002).
22. Weinberg, S.: The Quantum Theory of Fields, Volume 1: Foundations, Cambridge: Cambridge University Press (1995).
23. Paris M.G.A.: Quantum Estimation for Quantum Technology, International Journal of Quantum Information, 07(01), (2009)
24. Ferrie, C., Granade, C. E. & Cory, D. G. How to best sample a periodic probability distribution, or on the accuracy of Hamiltonian finding strategies. *Quantum Information Processing* **12**, 611–623. <https://doi.org/10.1007/s11128-012-0407-6> (2013).
25. Gough, J. E. & Belavkin, V. P. Quantum control and information processing. *Quantum Information Processing* **12**, 1397–1415. <https://doi.org/10.1007/s11128-012-0491-7> (2013).
26. Sun, J., Lu, S., Liu, F., Zhou, Q. & Zhang, Z. Generalized relation between fidelity and quantum adiabatic evolution. *Quantum Information Processing* **14**, 1757–1765. <https://doi.org/10.1007/s11128-015-0972-6> (2015).
27. Shor, P. W. Progress in Quantum Algorithms. *Quantum Information Processing* **3**, 1–5 (2004).
28. Schirmer, S. G., Kollı, A. & Oi, D. K. L. Experimental Hamiltonian identification for controlled two-level systems *Phys. Rev. A* **69**, 050306(R) (2004).
29. Leghtas, Z., Turinici, G., Rabitz, H. & Rouchon, P. Hamiltonian identification through enhanced observability utilizing quantum control. *Automatic Control, IEEE Transactions on* **57**(10), 2679–2683 (2012).
30. Moghadam, M. S., Nezamabadi, H. & Farsangi, M. M. A quantum inspired gravitational search algorithm for numerical function optimization. *Information Sciences* **267**, 83–100 (2014).
31. Deutsch, D. Jozsa R: Rapid solution of problems by quantum computation. *The Royal Society London Proceedings A* **439**, 553–558 (1992).
32. Gautam K. and Ahn C. W.: Quantum Path Integral Approach for Vehicle Routing Optimization with Limited Qubit”, *IEEE Transactions on intelligent transportation systems*, Vol. 25 (5), pp. 3244 - 3258, 06 December 2023. 10.1109/TITS.2023.3327157
33. Kumar, P. Direct implementation of an N-qubit controlled-unitary gate in a single step. *Quantum Information Processing* **12**, 1201–1223 (2013).
34. Peskin, M.E. (1995). An Introduction To Quantum Field Theory (1st ed.). CRC Press. <https://doi.org/10.1201/9780429503559>

## Acknowledgements

We would like to thank MEMI lab, GIST South Korea for providing facilities of this project work.

## Author contributions

The K.G provided the theoretical interpretation, wrote and reviewed the manuscript and C. W. Ahn elaborated some concepts with reviewed the text.

## Funding

This work was supported by Basic Science Research Program through the National Research Foundation of Korea (NRF) funded by the Korea government (MSIT) (RS-2024-00347902) and the Institute of Information & communications Technology Planning & Evaluation (IITP) grant funded by the Korea government (MSIT) (No.2019-0-01842, Artificial Intelligence Graduate School Program (GIST)).

## Declarations

### Conflicts of interest

On behalf of author, the corresponding author states that there is no conflict of interest.

### Additional information

**Correspondence** and requests for materials should be addressed to C.W.A.

**Reprints and permissions information** is available at [www.nature.com/reprints](http://www.nature.com/reprints).

**Publisher's note** Springer Nature remains neutral with regard to jurisdictional claims in published maps and institutional affiliations.

**Open Access** This article is licensed under a Creative Commons Attribution-NonCommercial-NoDerivatives 4.0 International License, which permits any non-commercial use, sharing, distribution and reproduction in any medium or format, as long as you give appropriate credit to the original author(s) and the source, provide a link to the Creative Commons licence, and indicate if you modified the licensed material. You do not have permission under this licence to share adapted material derived from this article or parts of it. The images or other third party material in this article are included in the article's Creative Commons licence, unless indicated otherwise in a credit line to the material. If material is not included in the article's Creative Commons licence and your intended use is not permitted by statutory regulation or exceeds the permitted use, you will need to obtain permission directly from the copyright holder. To view a copy of this licence, visit <http://creativecommons.org/licenses/by-nc-nd/4.0/>.

© The Author(s) 2024